Increased spatial heterogeneity in vegetation greenness due to vegetation greening in mainland China

Rui Yao[a], Lunche Wang[a,*], Xin Huang[b,c,*], Xinxin Chen[a], Zhengjia Liu[d]

[a] Laboratory of Critical Zone Evolution, School of Earth Sciences, China University of Geosciences, Wuhan 430074, China
[b] School of Remote Sensing and Information Engineering, Wuhan University, Wuhan 430079, China
[c] State Key Laboratory of Information Engineering in Surveying, Mapping and Remote Sensing, Wuhan University, Wuhan 430079, China
[d] Institute of Geographic Sciences and Natural Resources Research, Chinese Academy of Sciences, Beijing 100101, China

ARTICLE INFO

ABSTRACT

Spatial heterogeneity in vegetation greenness (VG) can influence earth surface process and resource ecology. However, its long-term change and driving forces remain poorly understood. In this study, MODIS enhanced vegetation index (EVI) data was used to examine the change in spatial heterogeneity in VG and its relationships with vegetation greening in mainland China during 2000–2017. Moving window standard deviation and range of growing season mean EVI (GSEVI) were used as proxies for spatial heterogeneity in VG. It was found that moving window standard deviation of GSEVI increased significantly over 33.8% to 53.7% of mainland China during 2000–2017, while it decreased significantly over less than 5% of mainland China. The results of moving window range of GSEVI were similar to moving window standard deviation of GSEVI. These may be explained by: (1) increased standard deviation and range of GSEVI accompanied by increased GSEVI value; and (2) faster greening speed in dense than in sparse vegetated areas. Additionally, the increased spatial heterogeneity in VG means the increased difference in VG between arid and humid regions, and between urban cores (UCs) and rural areas. These may primarily be attributed to slower greening speed in arid than in humid regions, and in UCs than in rural areas. Thus some benefits from vegetation greening may be much less in arid than in humid regions, and in UCs than in rural areas. Overall, this study analyzed an interesting phenomenon that vegetation greening may increase spatial heterogeneity in VG, which has a series of implications for environment and human activities.

1. Introduction

Vegetation plays a key role in terrestrial biosphere (e.g. regulating energy, carbon and water cycles) and can bring a large amount of positive effects to human society and surface environment (e.g. preventing soil erosion, mitigating green house effects, urban heat island and air pollution), thus vegetation dynamics is attracting increasingly interest (Myeong et al., 2006; Nowak et al., 2006; Oldfield et al., 2013; Pan et al., 2018; Qin et al., 2017; Wen et al., 2017; Yao et al., 2017b; Zhang et al., 2017). Satellite remote sensing is considered as one of the most important methods to monitor large-scale vegetation dynamics due primarily to its wide and full coverage, temporally continuous, and easy and free access. Satellite-based vegetation indices (VIs) for example normalized difference VI (NDVI) and enhanced VI (EVI) are based on different reflectance among bands. They can be used as proxies for vegetation greenness (VG) (or other parameters, e.g. productivity). High NDVI and EVI represent high VG (Huete et al., 2002).

One of the important properties of landscapes is spatial heterogeneity. Spatial heterogeneity in VG is related to habitat diversity, which can affect animal activity, species richness and ecosystem stability (Adler et al., 2001; Gould, 2000; John et al., 2008; Levin et al., 2007; Murwira and Skidmore, 2005; Parviainen et al., 2010). Studies have shown that the spatial heterogeneity in VIs were linked to species richness and animal activity (Fairbanks and McGwire, 2004; Gould, 2000; John et al., 2008; Levin et al., 2007; Seto et al., 2004). For example, Levin et al. (2007) found a positive relationship between plant species richness and spatial standard deviation of NDVI in Mount Hermon (Israel). Seto et al. (2004) showed that spatial mean, maximum and standard deviations of NDVI were all positively correlated with bird species richness at Great Basin of western North America. Murwira and Skidmore (2005) showed that spatial heterogeneity in NDVI was strongly related to elephant presence in Zimbabwe. However, to our knowledge, the long-term change of spatial heterogeneity in VG over a large area has not been documented in literature.

* Corresponding authors at: School of Geography and Information Engineering, China University of Geosciences, Wuhan 430074, China (L. Wang).
E-mail addresses: wang@cug.edu.cn (L. Wang), huang_whu@163.com (X. Huang).

Using satellite data, a large amount of studies showed that vegetation is greening from regional to global scales (Jiang et al., 2017; Pan et al., 2018; Piao et al., 2015; Wang et al., 2017; Zhang et al., 2017; Zhu et al., 2016). For example, Zhang et al. (2017) used Moderate Resolution Imaging Spectroradiometer (MODIS) data to show that global NDVI and EVI increased significantly for the period 2001–2015. Zhu et al. (2016) showed that significant increasing trends of leaf area index (LAI) were found over 25%–50% of the world during 1982–2009, which was mainly (70%) attributed to increased CO_2 in the atmosphere. Piao et al. (2015) showed that the LAI increased at the rate of 0.0070/ year (averaged for three LAI dataset) in China from 1982 to 2009. However, the responses of spatial heterogeneity in VG to vegetation greening are not clear. Thus, two questions were raised: (1) how does the spatial heterogeneity in VG change in past years? (2) Does vegetation greening affect the spatial heterogeneity in VG?

The purpose of this article is to answer above mentioned two questions. Mainland China covers a large area and has various climate and vegetation types. In addition, previous studies showed that the greening trend was more pronounced in mainland China than in other regions (Zhang et al., 2017; Zhu et al., 2016). These make mainland China an ideal region to investigate the change of spatial heterogeneity in VG and its relationships with vegetation greening. Additionally, the responses to vegetation greening in mainland China can be regarded as the "harbingers" of the future for other regions in the world. To solve above questions, this study analyzed: (1) the change of spatial heterogeneity in VG in mainland China during 2000–2017; (2) relationships between spatial heterogeneity in VG and vegetation greening; and (3) implications of change in spatial heterogeneity in VG.

2. Data and methods

2.1. Study area

The area of mainland China is approximately 9.6 million km², which ranked third in the world. Mainland China has various climate types ranging from humid and hot climate in southeast to cold and dry climate in northwest. In addition, vegetation differed greatly across mainland China, ranging from rainforests in southeast to deserts in northwest. The EVI gradually decreases from Southeast China to Northwest China (Fig. 1). Furthermore, urban samples in this study include 2 urban agglomerations (Yangtze River Delta urban agglomeration (YRD), including Shanghai, Changzhou, Wuxi and Suzhou; Pearl River Delta urban agglomeration (PRD), including Guangzhou, Dongguan, Foshan, Shenzhen, Zhongshan, Xianggang, Zhuhai and Jiangmen), 4 municipalities and 25 provincial capitals (Fig. 1).

2.2. Data

Vegetation greenness information was extracted from MODIS MOD13A3 EVI data (1000 m spatial resolution, monthly composite, version 6) from 2000 to 2017. 250 m spatial resolution MOD13Q1 EVI data (16-day composite, version 6) was utilized as a supplement (see Section 2.3). Compared with NDVI, EVI minimizes the effects of background reflectance variations. Thus it is more appropriate for monitoring vegetation dynamics in sparse vegetated areas for example urban areas (Huete et al., 2002; Zhang et al., 2004; Dallimer et al., 2011; Zhou et al., 2014). This study only analyzed the EVI in growing season (from April to October) to minimize the effects of winter snow (Yao et al., 2017b; Zhou et al., 2014). In addition, this study mainly focused on spatial heterogeneity in VG and deserts were not excluded. Negative EVI values were removed in this study.

Land cover information was obtained from China's Land Use/Cover Datasets (CLUDs) in the year 2000, 2005, 2010 and 2015. In this study, CLUDs were used to differentiate land cover types (see Section 3.2) and extract urban areas (see Section 2.3). CLUDs were produced from 30 m spatial resolution Landsat TM/ETM + and HJ-1A/1B data. The overall accuracy of CLUDs is greater than 90% for 25 land cover types. Detailed information, including data processing, accuracy assessment and classification information can be found in Kuang et al. (2016) and Liu et al. (2014).

2.3. Methods

In this study, MOD13A3 EVI data was mosaicked and reprojected using MODIS Reprojection Tool (MRT). Then the growing season mean EVI (GSEVI) in mainland China was calculated for each year. Spatial heterogeneity in VG at local scale was analyzed using moving window method. Moving window standard deviation and range of GSEVI were
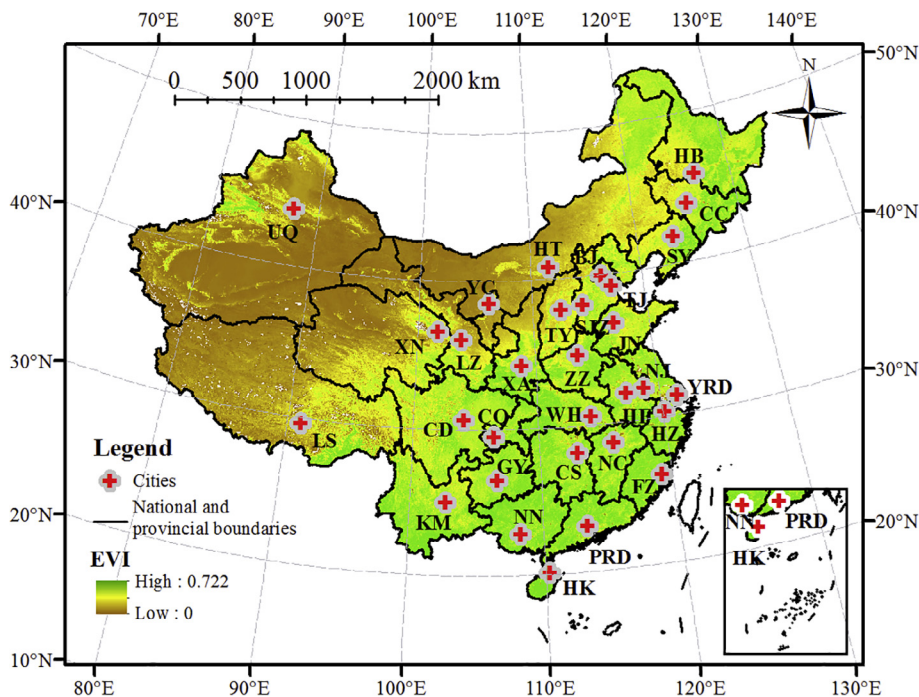
Fig. 1. Study area in this study. Background map is mean growing season mean enhanced vegetation index (GSEVI) during 2000–2002. HB: Harbin; CC: Changchun; UQ: Urumqi; SY: Shenyang; HT: Hohhot; BJ: Beijing; TJ: Tianjin; YC: Yinchuan; SJZ: Shijiazhuang; TY: Taiyuan; JN: Jinan; XN: Xining; LZ: Lanzhou; ZZ: Zhengzhou; XA: Xi'an; NJ: Nanjing; YRD: Yangtze River Delta urban agglomeration; HF: Heifei; HZ: Hangzhou; WH: Wuhan; CD: Chengdu; CQ: Chongqing; NC: Nanchang; CS: Changsha; FZ: Fuzhou; GY: Guiyang; KM: Kunming; NN: Nanning; PRD: Pearl River Delta urban agglomeration; HK: Haikou; LS: Lhasa.

Table 1

Proportions of significant (p < 0.05) increasing and decreasing trends of moving window standard deviation of growing season mean enhanced vegetation index (GSEVI) in mainland China during 2000–2017.

	9 * 9 pixel moving window	29 * 29 pixel moving window	49 * 49 pixel moving window	69 * 69 pixel moving window	89 * 89 pixel moving window
Significant increasing trend	33.8%	44.5%	49.0%	51.7%	53.7%
Significant decreasing trend	4.5%	3.3%	2.8%	2.5%	2.2%

used as proxies for spatial heterogeneity in VG. To ensure the robustness of the results, a total of 5 moving windows were used: 9 * 9, 29 * 29, 49 * 49, 69 * 69 and 89 * 89 pixel moving window. The spatial heterogeneity in VG in mainland China in each year can be mapped as follows: the value of central pixel of the window was given as the standard deviation or range of GSEVI in the window. After that, the trends of moving window standard deviation and range of GSEVI during 2000–2017 were calculated at the pixel level using Mann-Kendall trend test, which is a superior method for detecting trends and was recommended by World Meteorological Organization (WMO) (Mann, 1945; Kendall, 1975; Sen, 1968; Hisdal et al., 2001; Wu et al., 2008; Shadmani et al., 2012). To test the sensitivity of the results of changes in spatial heterogeneity in VG to the size of moving window, the MOD13Q1 data and above mentioned method were used. For the purposes of examining the relationships between vegetation greening and spatial heterogeneity in VG, the trends of moving window maximum and minimum GSEVI (using only MOD13A3 data) were calculated using the same method.

Trend of GSEVI (using only MOD13A3 data) from 2000 to 2017 was analyzed using Mann-Kendall trend test. Trends of GSEVI difference between dense and sparse vegetated areas at local scale were also analyzed using moving window method. In this study, dense and sparse vegetated areas were defined as mean GSEVI during 2000–2002 higher than 0.35 and lower than 0.15, respectively (both accounting for about one third of the area of mainland China). Other thresholds were utilized to test the robustness of the results (results see Section 3.2): (1) dense and sparse vegetated areas were defined as GSEVI higher than 0.3 and lower than 0.15, respectively; (2) dense and sparse vegetated areas were defined as GSEVI higher than 0.35 and lower than 0.1, respectively. GSEVI difference between dense and sparse vegetated areas in each year was mapped as follows: the value of central pixel in a window was given as the GSEVI difference between dense and sparse vegetated areas. After that, the Mann-Kendall trend test was applied to calculate the trends at the pixel level during 2000–2017. Furthermore, to examine the relationships between spatial heterogeneity in VG and vegetation greening, two types of Spearman's correlation analyses were performed: (1) spatial correlation analyses between slope of moving window standard deviation of GSEVI and slope of moving window mean GSEVI for the period 2000–2017 were performed across the whole mainland China; and (2) temporal correlation analyses between moving window standard deviation of GSEVI and moving window mean GSEVI were conducted at the pixel level across 2000–2017.

Percentage of urban area maps with spatial resolution of 1000 m (match MOD13A3 data) were generated from 30 m spatial resolution CLUDs in the year 2000, 2005, 2010 and 2015. To minimize the effects of urbanization on VG, this study examined the GSEVI (using only MOD13A3 data) trends in urban cores (UCs, those 1000 m spatial resolution pixels contain 100% of 30 m spatial resolution urban pixel

were first extracted from CLUDs in the year 2000, 2005, 2010 and 2015. Then the intersection areas were defined as UCs) in the selected 31 cities for the period 2000–2017. Note that the UCs does not necessarily mean it contains 100% of urban areas, since an original 30 m spatial resolution urban pixel may contain other land cover types (e.g. urban green spaces). In addition, 20–25 km buffers around urban areas (pixels with 50% of urban area in the year 2015) were employed as reference rural areas (removing pixels with urban area higher than 0% in any one of the four CLUDs). We used 20–25 km buffers because the footprint of urbanization may be larger than actual urban area size (Liu et al., 2015; Yao et al., 2018b; Zhou et al., 2016). To reduce the effects of climate variability, the rural areas were not set farther away from the urban areas (Yao et al., 2017a; Zhou et al., 2015). Trends of GSEVI in UCs and rural areas for the period 2000–2017 were computed using Mann-Kendall trend test.

3. Results and discussions

3.1. Change of spatial heterogeneity in VG

Spatial heterogeneity in VG changed significantly at both national and local scales in mainland China for the period 2000–2017. At national scale, the standard deviation of GSEVI across the whole mainland China increased significantly at the rate of 0.00132/year (p < 0.01). The standard deviations of GSEVI across mainland China averaged for 2000–2002 and 2015–2017 were 0.149 and 0.168, respectively. At local scale, significant (p < 0.05) increasing trends of standard deviation of GSEVI for 5 moving windows were observed over 33.8% to 53.7% of mainland China during 2000–2017, while significant decreasing trends were found over less than 5% of mainland China (Table 1). In addition, moving window range of GSEVI increased significantly over 31.3% to 54.0% of mainland China, whereas it declined significantly over less than 4% of mainland China (Table 2). Furthermore, the proportions of significant increasing trends of moving window standard deviation and range of GSEVI were much lower for 9 * 9 pixel moving window than other moving windows (Tables 1 and 2). Spatially, most areas in Southeast and Northwest China exhibited significant increasing trends of moving window standard deviation and range of GSEVI, while insignificant trends were mainly found in Tibetan Plateau and Northeast China (Figs. 2 and 3).

The minimum area of moving window of the MOD13A3 data is 81 km^2 (9 * 9 pixel moving window), which may still be too large in terms of analyzing species richness (Gould, 2000; Levin et al., 2007; Seto et al., 2004). In addition, it seems that the proportions of significant increasing trends of moving window standard deviation and range of GSEVI decrease significantly with decreasing window size (Tables 1 and 2). Thus 3 tiles (h25v05, h26v05 and h27v05, accounting for about 35.5% of area of the mainland China) 250 m spatial resolution

Table 2

Proportions of significant (p < 0.05) increasing and decreasing trends of moving window range of GSEVI for the period 2000–2017.

	9 * 9 pixel moving window	29 * 29 pixel moving window	49 * 49 pixel moving window	69 * 69 pixel moving window	89 * 89 pixel moving window
Significant increasing trend	31.3%	43.1%	48.9%	51.9%	54.0%
Significant decreasing trend	3.5%	2.5%	2.2%	2.1%	1.9%
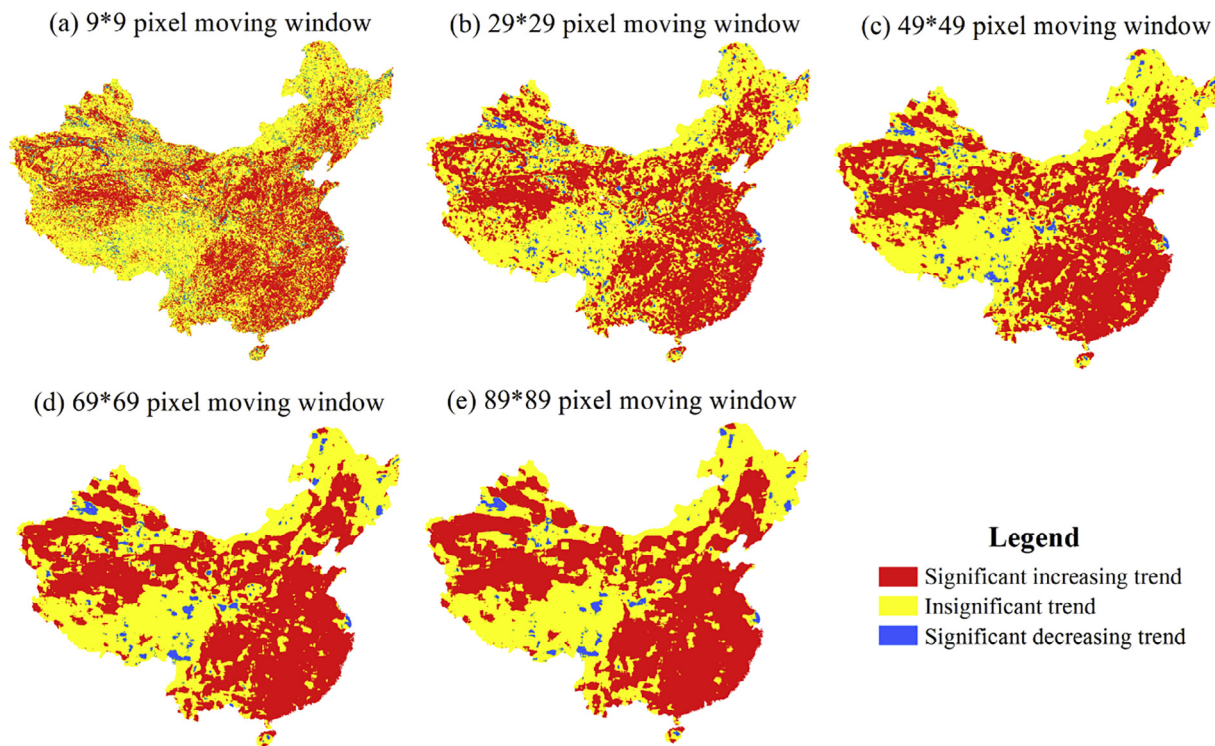
Fig. 2. Spatial distributions of trends of moving window standard deviation of GSEVI in mainland China for the period 2000–2017.

MOD13Q1 data were utilized as a supplement. Above mentioned 5 moving windows were applied, the areas of these windows of the MOD13Q1 data range from $5.06 \, \text{km}^2$ to $495.06 \, \text{km}^2$. Note that the minimum area of the moving window of MOD13A3 data ($81 \, \text{km}^2$) is within this range. Significant increasing trends of moving window standard deviation of GSEVI derived from MOD13Q1 data were observed over 35.5% to 50% of the study area (Fig. S1 and Table S1.

Similarly, the proportions of significant increasing trends of moving window range of GSEVI derived from MOD13Q1 data ranged from 33.5% to 50.1% (Fig. S2 and Table S2). In addition, the proportions of significant increasing trends of moving window standard deviation and range of GSEVI derived from MOD13Q1 data were much lower for 9 * 9 pixel moving window than other moving windows (Tables S1 and S2). It suggested that the results of trends of moving window standard
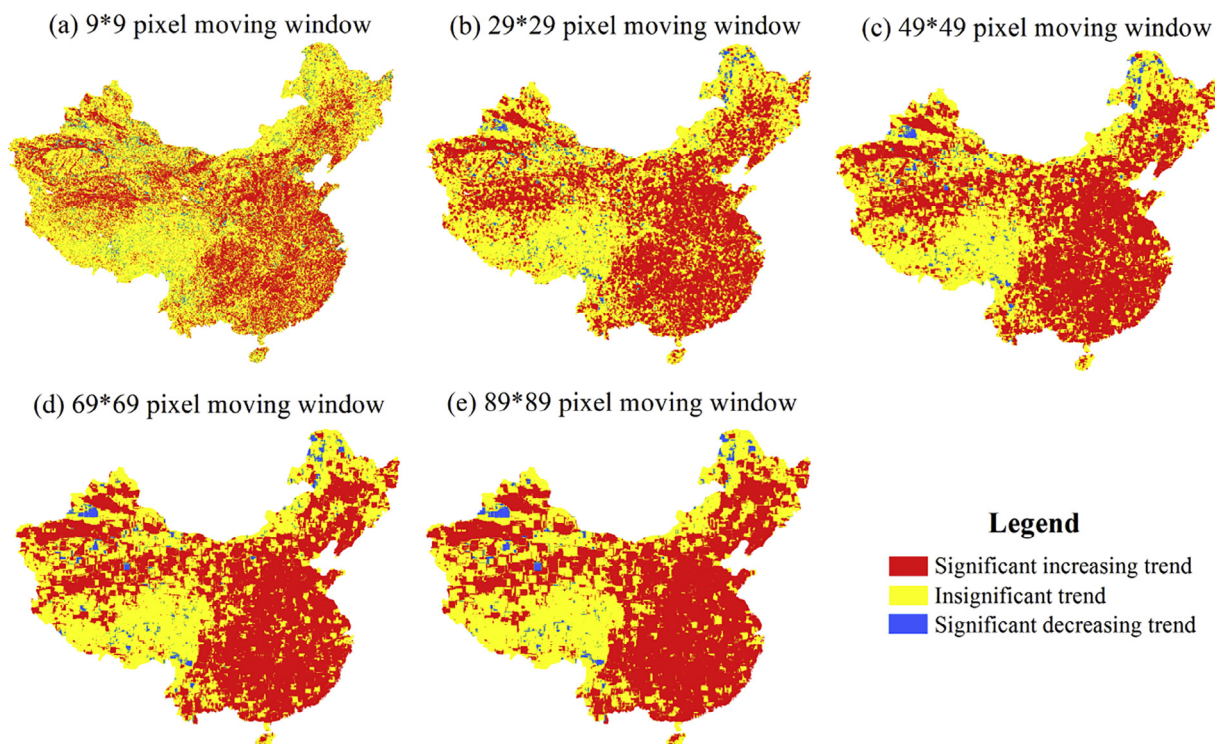
Fig. 3. Spatial distributions of trends of moving window range of GSEVI during 2000–2017.
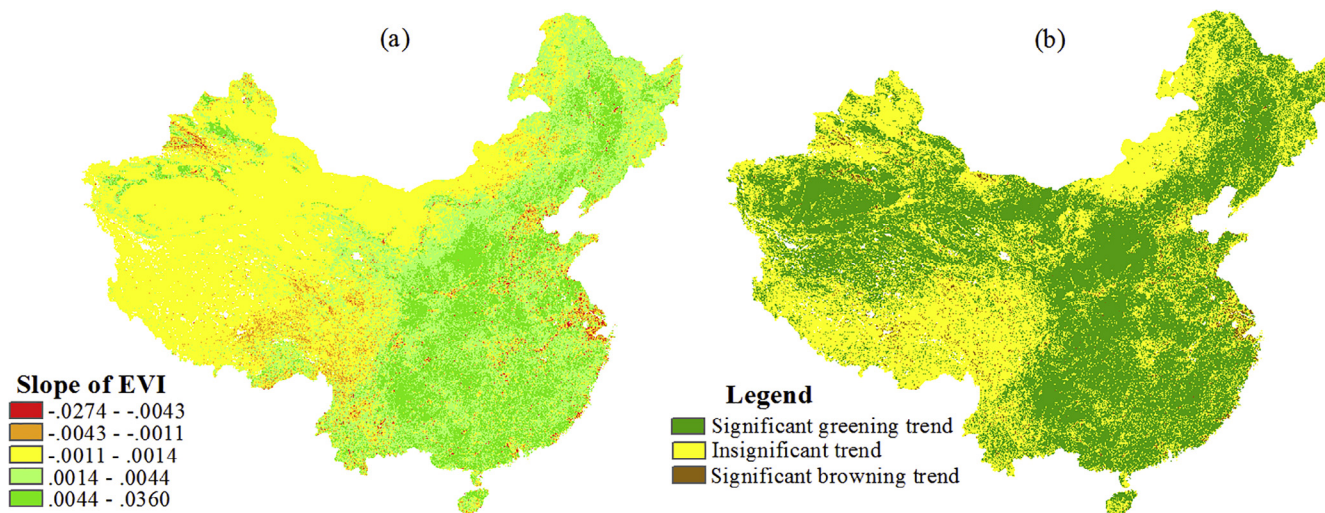
Fig. 4. Trends of GSEVI in China mainland during 2000–2017: (a) slope; (b) significance level.
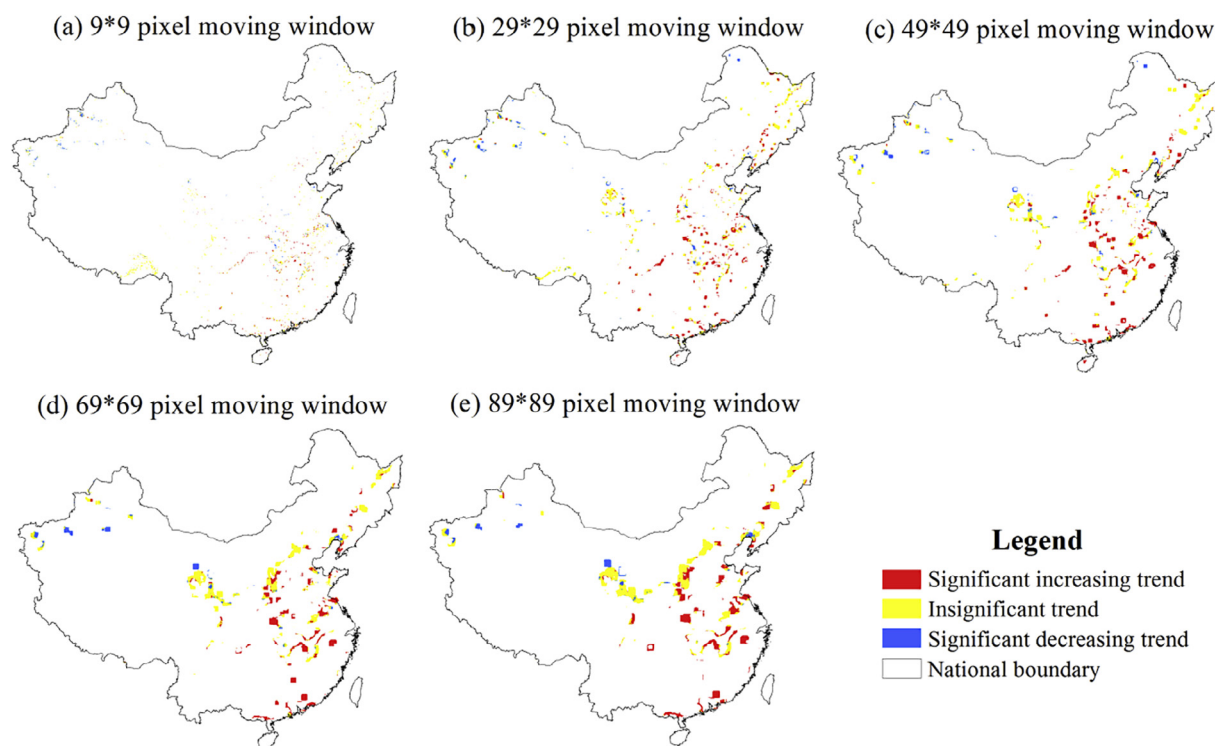
Fig. 5. Spatial distributions of trends of moving window GSEVI difference between dense and sparse vegetated areas in windows with increasing rate of GSEVI higher than 90%.

deviation and range of GSEVI may be sensitive to the number of pixels of the window rather than the area of the window.

Many studies have shown that spatial standard deviation of VG was positively related to species richness, which is defined as the number of species in a community and is an indicator for ecosystem stability (Fairbanks and McGwire, 2004; Gould, 2000; John et al., 2008; Levin et al., 2007; Seto et al., 2004). This is because areas with high spatial heterogeneity in VG can provide various landscapes to allow various species to survive. For a specific species, high spatial heterogeneity in VG can increase the probability that specific resources (e.g. water resources, sunshine, food, shelter and breeding ground) will be available (Seto et al., 2004). Thus the increased spatial heterogeneity in VG may have positive effects on species richness.

3.2. Relationships between spatial heterogeneity in VG and vegetation greening

Trends of GSEVI in China mainland for the period 2000–2017 were shown in Fig. 4. Significant increasing and decreasing trends of GSEVI during 2000–2017 were observed over 53.1% and 1.8% of China mainland, respectively. For the whole China mainland averaged, the GSEVI increased at the rate of 0.00191/year (p < 0.01). The GSEVI averaged for 2000–2002 and 2015–2017 in mainland China were 0.235 and 0.264, respectively. Spatially, compared with Northwest China, Southeast China showed higher increasing rate of GSEVI during 2000–2017. In addition, as mentioned in Section 3.1, Southeast China exhibited higher mean GSEVI during 2000–2002 than Northwest China. Thus the GSEVI difference between Southeast and Northwest China

Table 3

Proportions of significant (p < 0.05) increasing and decreasing trends of moving window GSEVI difference between dense and sparse vegetated areas in windows with increasing rate of GSEVI higher than 90%.

	9 * 9 pixel moving window (n = 83,873)	29*29 pixel moving window (n = 252,338)	49*49 pixel moving window (n = 333,883)	69*69 pixel moving window (n = 376,714)	89*89 pixel moving window (n = 432,506)
Significant increasing trend	22.4%	35.6%	37.5%	35.5%	36.5%
Significant decreasing trend	13.2%	11.2%	9.5%	9.1%	8.1%

increased during 2000–2017. That may be the primary reason for the increased spatial heterogeneity in VG at national scale. Furthermore, insignificant trends of GSEVI were mainly found in Tibetan Plateau (Fig. 4), which was consistent with the trends of moving window standard deviation and range of GSEVI (Figs. 2 and 3). The spatial distribution of slope of GSEVI was similar to previous studies (Piao et al., 2015; Zhang et al., 2017).

Dense vegetated areas generally showed faster greening trends than sparse vegetated areas. At national scale, Southeast China has higher mean GSEVI during 2000–2002 and higher increasing rate of GSEVI during 2000–2017 (Figs. 1 and 4). In addition, the increasing rates of dense and sparse vegetated areas for the whole mainland China were 0.00328/year (p < 0.01) and 0.00070/year (p < 0.01), respectively. At local scale, the trends of moving window GSEVI difference between dense and sparse vegetated areas were calculated. Note that: (1) windows with dense or sparse vegetated pixels lower than 1% were excluded; and (2) windows with the proportion of increasing rate of GSEVI lower than 90% were excluded, since the purpose was to investigate the changes in GSEVI difference between dense and sparse vegetated areas in response to vegetation greening. The moving window GSEVI difference between dense and sparse vegetated areas increased significantly in 22.4%–36.5% of the total samples for the period 2000–2017, while it decreased significantly in 8.1%–13.2% of the total samples (Fig. 5 and Table 3). In addition, other thresholds were used as supplements, and similar results were observed (Tables S3 and S4). These suggested that vegetation greening may significantly increase the difference in VG between dense and sparse vegetated areas, and the speed of greening was generally faster in dense than in sparse vegetated areas. The amount of vegetation is more in dense than in sparse vegetated areas. More vegetation will be affected by driving forces (e.g. climate and human activity) in dense than in sparse vegetated areas. Thus the interannual changes in GSEVI may be larger, and the greening speed may be faster in dense than in sparse vegetated areas (except land cover change) (Yao et al., 2018a). For example, the GSEVI of dense and sparse vegetated areas were 0.4 and 0.1, respectively, in the year 2000. The GSEVI of both dense and sparse vegetated areas increased 10% from 2000 to 2017. Thus the increment of dense vegetated areas (0.04) was much higher than sparse vegetated areas (0.01), and the GSEVI difference between dense and sparse vegetated areas increased by 0.03.

The increased spatial heterogeneity in VG may primarily be attributed to vegetation greening. The slope of moving window mean GSEVI was significantly and positively correlated with slope of moving window standard deviation of GSEVI across the entire China mainland (9 * 9 pixel moving window: r = 0.492, p < 0.01; 29 * 29 pixel moving window: r = 0.595, p < 0.01; 49 * 49 pixel moving window: r = 0.637, p < 0.01; 69 * 69 pixel moving window: r = 0.662, p < 0.01; 89 * 89 pixel moving window: r = 0.675, p < 0.01). This suggested that regions with faster greening speed generally showed faster increasing rate of spatial heterogeneity in VG. In addition, moving window mean GSEVI was significantly and positively correlated with moving window standard deviation of GSEVI across 2000–2017 over 47.3%–71.9% of mainland China (Fig. 6 and Table 4). Thus years with high GSEVI normally exhibited high spatial heterogeneity in VG. These phenomena can be explained by two points. Firstly, from the perspective of statistics, high value generally shows high standard deviation. This is why the coefficient of variation (CV, standard deviation divided by mean) is raised. It was found that the moving window CV of GSEVI increased significantly over 17.0%–22.6% of mainland China, which was only a little higher than significant decreasing trend (14.3%–16.3%; Fig. 7 and Table 5). Secondly, as shown in Fig. 5 and Table 3, dense vegetated areas generally showed higher increasing rate of GSEVI than sparse vegetated areas. Further analyses showed that the proportions of significant increasing trends of moving window maximum GSEVI were much higher than minimum GSEVI (Tables S5 and S6). These may increase the GSEVI difference between dense and sparse

(a) 9*9 pixel moving window   (b) 29*29 pixel moving window   (c) 49*49 pixel moving window

(d) 69*69 pixel moving window   (e) 89*89 pixel moving window

Legend
- Significant positive correlation
- Insignificant trend
- Significant negative correlation
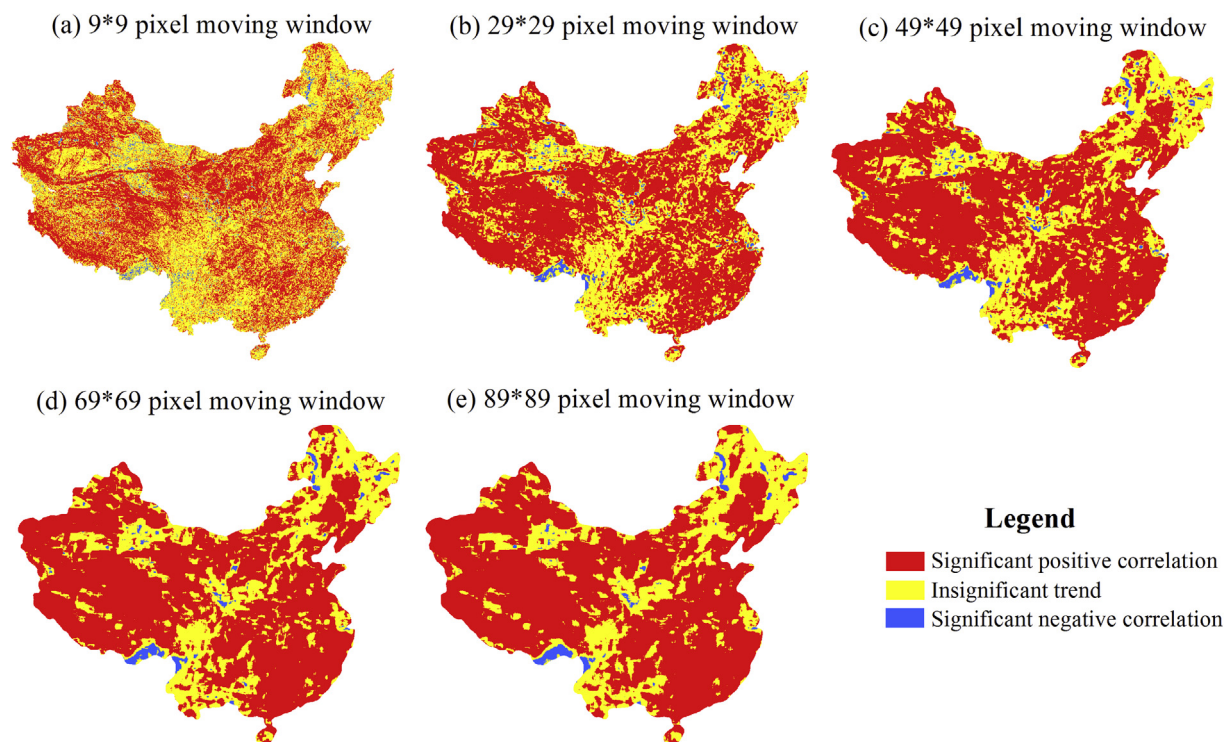
Fig. 6. Spatial distributions of correlation coefficients between moving window mean GSEVI and moving window standard deviation of GSEVI across 2000–2017.

Table 4

Proportions of significant ($p < 0.05$) positive and negative correlations between moving window mean GSEVI and moving window standard deviation of GSEVI across 2000–2017.

	9 * 9 pixel moving window	29 * 29 pixel moving window	49 * 49 pixel moving window	69 * 69 pixel moving window	89 * 89 pixel moving window
Significant positive correlation	47.3%	62.5%	67.7%	70.1%	71.9%
Significant negative correlation	2.6%	2.1%	1.9%	1.7%	1.6%

vegetated areas and be the major reason for the increased moving window standard deviation and range of GSEVI.

Significant positive correlations between moving window mean GSEVI and moving window standard deviation of GSEVI across 2000–2017 were found in over 47.3%–71.9% of China mainland (Fig. 6 and Table 4). However, some regions showed significant negative correlations (e.g. Northeast China, Southwest China and Central China; Figs. 6 and 8). For regions with significant negative correlations in Northeast and Central China, woodland generally have higher mean GSEVI during 2000–2002 but lower slopes of GSEVI during 2000–2017 than cropland (Fig. 8(b)–(g)). The higher increasing rate of cropland may be attributed to human activities (e.g. improved agricultural technologies). Thus the GSEVI differences between cropland and woodland decreased, and the spatial heterogeneity in VG declined as vegetation greening. For regions with significant negative correlations in Southwest China, areas showed higher slopes of GSEVI during 2000–2017 generally have lower mean GSEVI during 2000–2002 (Fig. 8(h)–(j)). Therefore, the spatial heterogeneity in VG declined as vegetation greening. This may be explained by global warming. In this region, areas showed high slopes of GSEVI during 2000–2017 generally have high altitude (derived from elevation data, not shown). As global warming, ice and snow in high altitude melt, thus the growing season of vegetation was prolonged and the GSEVI increased significantly. Finally, the GSEVI difference between dense and sparse vegetated areas decreased and the spatial heterogeneity in VG declined in this region.

3.3. Implications of the increased spatial heterogeneity in VG

3.3.1. Increased difference in VG between arid and humid regions

In this study, the GSEVI difference between humid Southeast and arid Northwest China significantly increased. The underlying mechanism was different vegetation greening speed. It is well known that vegetation can decrease temperature through transpiration. Zeng et al. (2017) found that global vegetation greening has retarded the increase in global air temperature by $0.09 \pm 0.02\,°C$ over the past 30 years. Previous studies showed that the speed of global warming was faster in arid than in humid regions (Huang et al., 2017). Unfortunately, slow greening speed may have little mitigation effects on global warming in arid Northwest China. In addition, other benefits brought about by vegetation greening may also be less significant in arid Northwest China than in humid Southeast China.

3.3.2. Increased difference in VG between UCs and rural areas

In Section 3.2, we found that the difference in VG between dense and sparse vegetated areas generally increased. We inferred that the difference in VG between UCs and rural areas may also increase, since UCs normally have less vegetation than rural areas.

The increasing trends of GSEVI in UCs and rural areas were observed in 30 of 31 cities (Fig. 9 and Table S7). However, the slopes of GSEVI in UCs were lower than in rural areas in 23 of 31 cities. For 31 cities averaged, the trends of GSEVI in UC and rural area were 0.00213 ± 0.00107/year and 0.00341 ± 0.00168/year, respectively. The numbers of cities with increasing rate of GSEVI higher than 0.004/

(a) 9*9 pixel moving window   (b) 29*29 pixel moving window   (c) 49*49 pixel moving window

(d) 69*69 pixel moving window   (e) 89*89 pixel moving window

Legend

■ Significant positive correlation
■ Insignificant correlation
■ Significant negative correlation
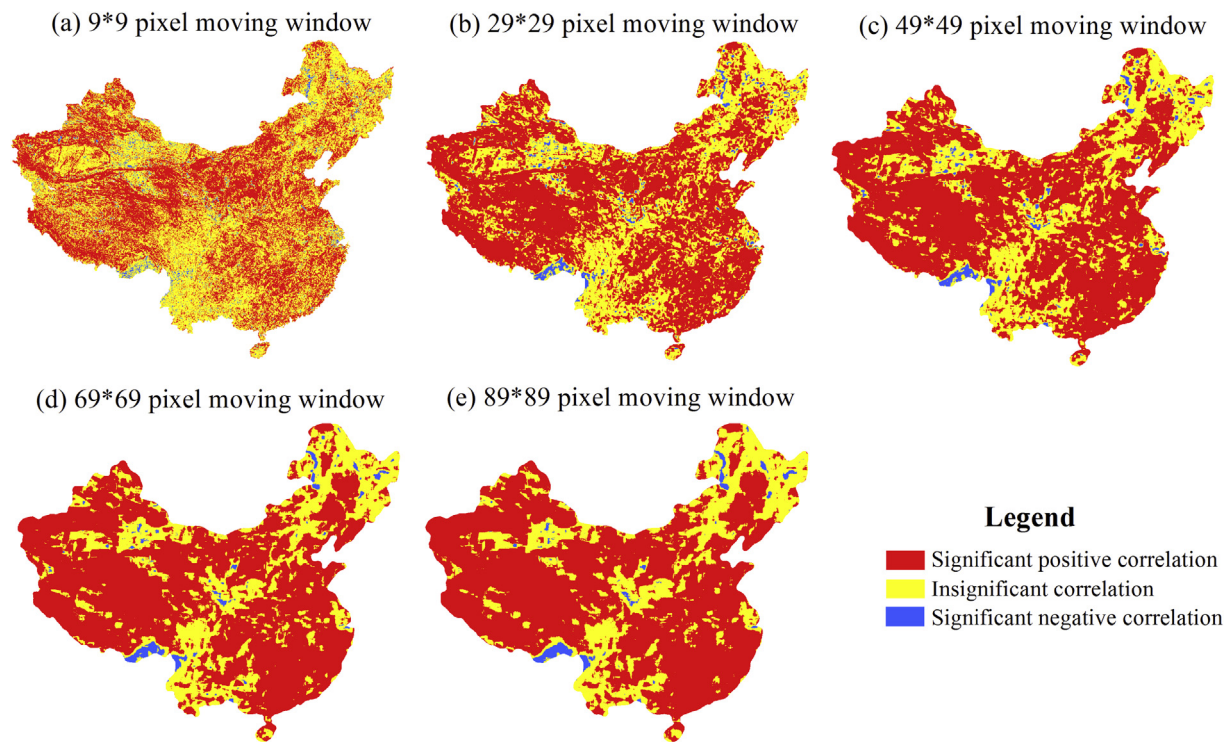
Fig. 7. Spatial distributions of trends of moving window coefficient of variation (CV) of GSEVI for the period 2000–2017.

Table 5
Proportions of significant (p < 0.05) increasing and decreasing trends of moving window coefficient of variation (CV) of GSEVI during 2000–2017.

	9 * 9 pixel moving window	29 * 29 pixel moving window	49 * 49 pixel moving window	69 * 69 pixel moving window	89 * 89 pixel moving window
Significant increasing trend	17.0%	20.5%	21.7%	22.2%	22.6%
Significant decreasing trend	14.3%	16.3%	16.5%	16.5%	16.3%

year in UCs and rural areas were 1 and 12, respectively (Tables S7). These results suggested that the speed of vegetation greening in UCs were generally slower than in rural areas, and the vegetation greening may increase the difference in VG between UCs and rural areas. This is possibly because the amount of vegetation is generally higher in UCs than in rural areas. The increased difference in VG between UCs and rural areas may be one of the potential driving factors of the increased spatial heterogeneity in VG at the local scale. Note that there were 8 cities with higher increasing trends of GSEVI in UCs than in rural areas. This can be attributed to many factors (e.g. background climate and human activities). For example, Yinchuan and Urumqi are surrounded by sparse vegetated areas and the rural GSEVI is low. Thus the rural GSEVI increased slowly in these two cities (Table S7). Hangzhou and Chengdu have much higher increasing rates of GSEVI in UCs than other cities. This may be attributed to effective greening policies in these two cities.

Vegetation is an important component of urban ecosystems. Urban vegetation can decrease local temperature and alleviate urban heat island through transpiration and posing a shading effect (Peng et al., 2012; Yao et al., 2017b, 2018c), reduce noise pollution through up-taking acoustic energy (Fang and Ling, 2003), and mitigate air pollution primarily by uptake via leaf stomata and improve urban air quality (Nowak et al., 2006; Salmond et al., 2013). In this study, we restricted the study area in pixels with 100% of the urban area. In addition, Chinese government has formulated a series of policies to preserve and create urban green spaces in recent decades (Zhao et al., 2013; Zhou et al., 2014; Zhou and Wang, 2011). Thus, the negative effects of urbanization on VG were minimized, while the positive effects of greening

policies on VG were retained. However, the present study showed that the increasing rate of GSEVI in UC was still much slower than in rural area averaged for 31 cities during 2000–2017. A series of benefits brought about by vegetation greening may be more pronounced in rural areas than in UCs. In addition, GSEVI in UCs is generally lower than in rural areas. Thus the GSEVI difference between UCs and rural areas increased due to vegetation greening. Previous studies used ΔEVI (urban EVI minus rural EVI) to reflect urbanization effects on VG (Yao et al., 2017a; Zhou et al., 2014), which may lead to inaccurate results in regions with fast vegetation greening trend, since the increased EVI difference between urban and rural areas may be caused by vegetation greening rather than urbanization.

4. Conclusions

In this study, MODIS EVI data were used to analyze the change in spatial heterogeneity in VG and its relationship with vegetation greening in mainland China for the period 2000–2017. Results showed that the proportions of significant increasing trend of moving window standard deviation (from 33.8% to 53.7%) and range (from 31.3% to 54.0%) of GSEVI were much higher than significant decreasing trend (less than 5%). The increase in spatial heterogeneity in VG can be explained from the perspective of mathematical statistics, and by faster greening speed in dense than in sparse vegetated areas. Additionally, greening speed may be slower in arid than in humid regions, and in UCs than in rural areas. Thus some benefits from vegetation greening may be much less in arid than in humid regions, and in UCs than in rural areas.
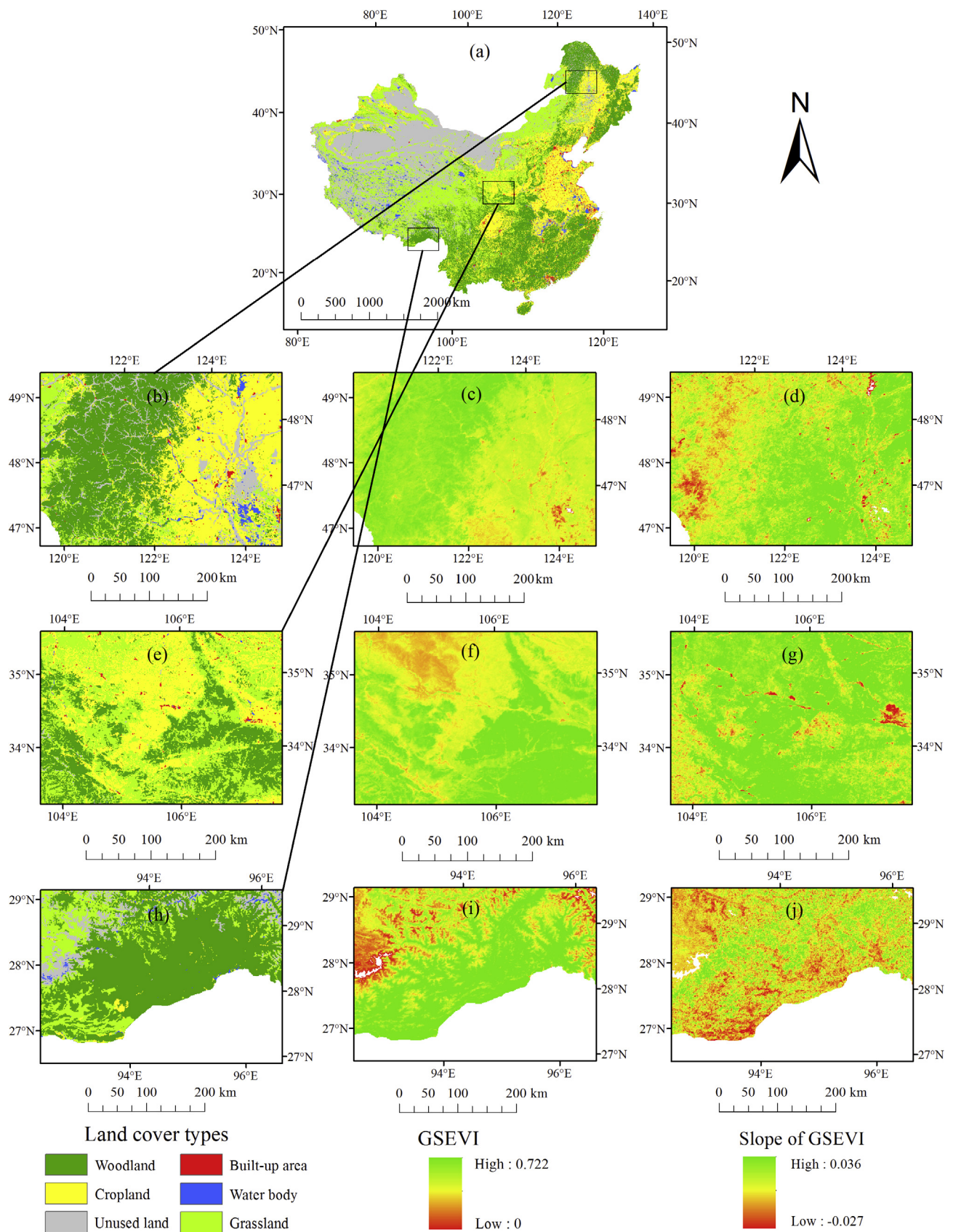
Fig. 8. Land cover maps in 2015 in: (a) mainland China; (b) Northeast China; and (e) Central China; (h) Southeast China. Mean GSEVI during 2000–2002 in: (c) Northeast China; (f) Central China; and (i) Southeast China. Slopes of GSEVI during 2000–2017 in: (d) Northeast China; (g) Central China; and (j) Southeast China.
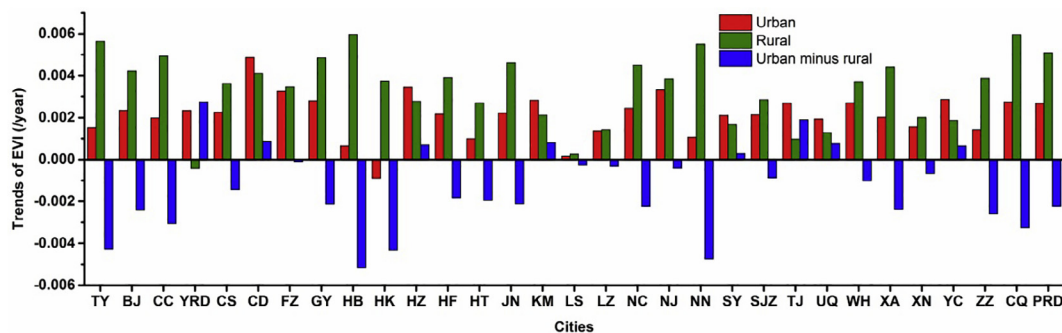
Fig. 9. Trends of GSEVI in 31 major Chinese cities for the period 2000–2017.

Overall, this study revealed an interesting finding and can enhance our understanding of the interactions between vegetation dynamic and surface ecological environment. Future studies can (1) examine the changes in spatial heterogeneity in VG in other regions; (2) using higher spatial resolution data to evaluate the contributions of different factors to the vegetation greenness change in urban area; and (3) further analyze and validate the impacts of increased spatial heterogeneity in VG on human society.

Appendix A. Supplementary data

Supplementary data to this article can be found online at https://doi.org/10.1016/j.ecolind.2018.12.039.

References

Adler, P., Raff, D., Lauenroth, W., 2001. The effect of grazing on the spatial heterogeneity of vegetation. Oecologia 128, 465–479.

Dallimer, M., Tang, Z., Bibby, P.R., Brindley, P., Gaston, K.J., Davies, Z.G., 2011. Temporal changes in greenspace in a highly urbanized region. Biol. Lett. 7, 763–766.

Fairbanks, D.H.K., McGwire, K.C., 2004. Patterns of floristic richness in vegetation communities of California: regional scale analysis with multi-temporal NDVI. Global Ecol. Biogeogr. 13, 221–235.

Fang, C.-F., Ling, D.-L., 2003. Investigation of the noise reduction provided by tree belts. Landscape Urban Plann. 63, 187–195.

Gould, W., 2000. Remote sensing of vegetation, plant species richness, and regional biodiversity hotspots. Ecol. Appl. 10 (6), 1861–1870.

Hisdal, H., Stahl, K., Tallaksen, L.M., Demuth, S., 2001. Have streamflow droughts in Europe become more severe or frequent. Int. J. Climatol. 21, 317–333.

Huang, J., Li, Y., Fu, C., Chen, F., Fu, Q., Dai, A., Shinoda, M., Ma, Z., Guo, W., Li, Z., Zhang, L., Liu, Y., Yu, H., He, Y., Xie, Y., Guan, X., Ji, M., Lin, L., Wang, S., Yan, H., Wang, G., 2017. Dryland climate change: recent progress and challenges. Rev. Geophys. 55, 719–778.

Huete, A., Didan, K., Miura, T., Rodriguez, E.P., Gao, X., Ferreira, L.G., 2002. Overview of the radiometric and biophysical performance of the MODIS vegetation indices. Remote Sens. Environ. 83, 195–213.

Jiang, C., Ryu, Y., Fang, H., Myneni, R., Claverie, M., Zhu, Z., 2017. Inconsistencies of interannual variability and trends in long-term satellite leaf area index products. Global Change Biol. 23, 4133–4146.

John, R., Chen, J., Lu, N., Guo, K., Liang, C., Wei, Y., Noormets, A., Ma, K., Han, X., 2008. Predicting plant diversity based on remote sensing products in the semi-arid region of Inner Mongolia. Remote Sens. Environ. 112, 2018–2032.

Kendall, M.G., 1975. Rank Correlation Methods. Griffin, London.

Kuang, W., Liu, J., Dong, J., Chi, W., Zhang, C., 2016. The rapid and massive urban and industrial land expansions in China between 1990 and 2010: a CLUD-based analysis of their trajectories, patterns, and drivers. Landscape Urban Plann. 145, 21–33.

Levin, N., Shmida, A., Levanoni, O., Tamari, H., Kark, S., 2007. Predicting mountain plant richness and rarity from space using satellite-derived vegetation indices. Divers. Distrib. 13, 692–703.

Liu, J., Kuang, W., Zhang, Z., Xu, X., Qin, Y., Ning, J., Zhou, W., Zhang, S., Li, R., Yan, C., Wu, S., Shi, X., Jiang, N., Yu, D., Pan, X., Chi, W., 2014. Spatiotemporal characteristics, patterns, and causes of land-use changes in China since the late 1980s. J. Geogr. Sci. 24, 195–210.

Liu, Y., Wang, Y., Peng, J., Du, Y., Liu, X., Li, S., Zhang, D., 2015. Correlations between urbanization and vegetation degradation across the World's metropolises using DMSP/OLS nighttime light data. Remote Sens. 7, 2067–2088.

Mann, H.B., 1945. Nonparametric tests against trend. Econometrica 13, 245–259.

MODIS Reprojection Tool V4.1 Software. Available online: https://lpdaac.usgs.gov/tools/modis_reprojection_tool (accessed on 31 January 2016).

Murwira, A., Skidmore, A.K., 2005. The response of elephants to the spatial heterogeneity of vegetation in a Southern African agricultural landscape. Landscape Ecol. 20, 217–234.

Myeong, S., Nowak, D.J., Duggin, M.J., 2006. A temporal analysis of urban forest carbon storage using remote sensing. Remote Sens. Environ. 101, 277–282.

Nowak, D.J., Crane, D.E., Stevens, J.C., 2006. Air pollution removal by urban trees and shrubs in the United States. Urban For. Urban Greening 4, 115–123.

Oldfield, E.E., Warren, R.J., Felson, A.J., Bradford, M.A., Bugmann, H., 2013. Challenges and future directions in urban afforestation. J. Appl. Ecol n/a–n/a.

Pan, N., Feng, X., Fu, B., Wang, S., Ji, F., Pan, S., 2018. Increasing global vegetation browning hidden in overall vegetation greening: insights from time-varying trends. Remote Sens. Environ. 214, 59–72.

Parviainen, M., Luoto, M., Heikkinen, R.K., 2010. NDVI-based productivity and heterogeneity as indicators of plant-species richness in boreal landscapes. Boreal Environ. Res. 15, 301–318.

Peng, S., Piao, S., Ciais, P., Friedlingstein, P., Ottle, C., Breon, F.M., Nan, H., Zhou, L., Myneni, R.B., 2012. Surface urban heat island across 419 global big cities. Environ. Sci. Technol. 46, 696–703.

Piao, S., Yin, G., Tan, J., Cheng, L., Huang, M., Li, Y., Liu, R., Mao, J., Myneni, R.B., Peng, S., Poulter, B., Shi, X., Xiao, Z., Zeng, N., Zeng, Z., Wang, Y., 2015. Detection and attribution of vegetation greening trend in China over the last 30 years. Global Change Biol. 21, 1601–1609.

Qin, Y., Xiao, X., Dong, J., Zhou, Y., Wang, J., Doughty, R.B., Chen, Y., Zou, Z., Moore, B., 2017. Annual dynamics of forest areas in South America during 2007–2010 at 50-m spatial resolution. Remote Sens. Environ. 201, 73–87.

Salmond, J.A., Williams, D.E., Laing, G., Kingham, S., Dirks, K., Longley, I., Henshaw, G.S., 2013. The influence of vegetation on the horizontal and vertical distribution of pollutants in a street canyon. Sci. Total Environ. 443, 287–298.

Sen, P.K., 1968. Estimates of the regression coefficient based on Kendall's tau. J. Am. Stat. Assoc. 63, 1379–1389.

Seto, K.C., Fleishman, E., Fay, J.P., Betrus, C.J., 2004. Linking spatial patterns of bird and butterfly species richness with Landsat TM derived NDVI. Int. J. Remote Sens. 25, 4309–4324.

Shadmani, M., Marofi, S., Roknian, M., 2012. Trend analysis in reference evapotranspiration using Mann-Kendall and Spearman's rho tests in arid regions of Iran. Water Resour. Manage. 26, 211–224.

Wang, X., Wang, T., Liu, D., Guo, H., Huang, H., Zhao, Y., 2017. Moisture-induced greening of the South Asia over the past three decades. Global Change Biol. 23, 4995–5005.

Wen, Z., Wu, S., Chen, J., Lu, M., 2017. NDVI indicated long-term interannual changes in vegetation activities and their responses to climatic and anthropogenic factors in the Three Gorges Reservoir Region, China. Sci. Total Environ. 574, 947–959.

Wu, H., Soh, L.K., Samal, A., Chen, X.H., 2008. Trend analysis of streamflow drought events in Nebraska. Water Resour. Manage. 22, 145–164.

Yao, R., Wang, L., Gui, X., Zheng, Y., Zhang, H., Huang, X., 2017a. Urbanization effects on vegetation and surface urban heat Islands in China's Yangtze River Basin. Remote Sens. 9, 540.

Yao, R., Wang, L., Huang, X., Chen, J., Li, J., Niu, Z., 2018a. Less sensitive of urban surface to climate variability than rural in Northern China. Sci. Total Environ. 628–629, 650–660.

Yao, R., Wang, L., Huang, X., Niu, Y., Chen, Y., Niu, Z., 2018b. The influence of different data and method on estimating the surface urban heat island intensity. Ecol. Indic. 89, 45–55.

Yao, R., Wang, L., Huang, X., Niu, Z., Liu, F., Wang, Q., 2017b. Temporal trends of surface urban heat islands and associated determinants in major Chinese cities. Sci. Total Environ. 609, 742–754.

Yao, R., Wang, L., Huang, X., Zhang, W., Li, J., Niu, Z., 2018c. Interannual variations in

surface urban heat island intensity and associated drivers in China. J. Environ. Manage. 222, 86–94.

Zeng, Z., Piao, S., Li, L.Z.X., Zhou, L., Ciais, P., Wang, T., Li, Y., Lian, X., Wood, E.F., Friedlingstein, P., Mao, J., Estes, L.D., Myneni, Ranga B., Peng, S., Shi, X., Seneviratne, S.I., Wang, Y., 2017. Climate mitigation from vegetation biophysical feedbacks during the past three decades. Nat. Clim. Change 7, 432–436.

Zhang, X., Friedl, M.A., Schaaf, C.B., Strahler, A.H., Schneider, A., 2004. The footprint of urban climates on vegetation phenology. Geophys. Res. Lett. 31, L12209.

Zhang, Y., Song, C., Band, L.E., Sun, G., Li, J., 2017. Reanalysis of global terrestrial vegetation trends from MODIS products: browning or greening? Remote Sens. Environ. 191, 145–155.

Zhao, J., Chen, S., Jiang, B., Ren, Y., Wang, H., Vause, J., Yu, H., 2013. Temporal trend of green space coverage in China and its relationship with urbanization over the last two decades. Sci. Total Environ. 442, 455–465.

Zhou, D., Zhao, S., Liu, S., Zhang, L., 2014. Spatiotemporal trends of terrestrial vegetation activity along the urban development intensity gradient in China's 32 major cities. Sci. Total Environ. 488–489, 136–145.

Zhou, D., Zhao, S., Zhang, L., Liu, S., 2016. Remotely sensed assessment of urbanization effects on vegetation phenology in China's 32 major cities. Remote Sens. Environ. 176, 272–281.

Zhou, D., Zhao, S., Zhang, L., Sun, G., Liu, Y., 2015. The footprint of urban heat island effect in China. Sci. Rep. 5, 11160.

Zhou, X., Wang, Y.-C., 2011. Spatial–temporal dynamics of urban green space in response to rapid urbanization and greening policies. Landscape Urban Plann. 100, 268–277.

Zhu, Z., Piao, S., Myneni, R.B., Huang, M., Zeng, Z., Canadell, J.G., Ciais, P., Sitch, S., Friedlingstein, P., Arneth, A., Cao, C., Cheng, L., Kato, E., Koven, C., Li, Y., Lian, X., Liu, Y., Liu, R., Mao, J., Pan, Y., Peng, S., Peñuelas, J., Poulter, B., Pugh, T.A.M., Stocker, B.D., Viovy, N., Wang, X., Wang, Y., Xiao, Z., Yang, H., Zaehle, S., Zeng, N., 2016. Greening of the Earth and its drivers. Nat. Clim. Change 6, 791–795.